Preparation and crystal structure of tetraoctylphosphonium tetrakis(pentafluorophenyl)borate ionic liquid for electrochemistry at its interface with water

Jane Stockmann, Paul Boyle, Zhifeng Ding

▶ To cite this version:

HAL Id: hal-01974488

https://hal-univ-diderot.archives-ouvertes.fr/hal-01974488

Submitted on 8 Jan 2019

Preparation and crystal structure of tetraoctylphosphonium tetrakis(pentafluorophenyl)borate ionic liquid for electrochemistry at its interface with water[†]

T. Jane Stockmann,[a,b] Paul D. Boyle[b] and Zhifeng Ding[b,∗]

[a]Sorbonne Paris Cité, Paris Diderot University, Interfaces, Traitements, Organisation et Dynamique des Systèmes, CNRS-UMR 7086, 15 rue J.A. Baïf, 75013 Paris, France.

[b]Center for Advanced Materials and Biomaterials Research (CAMBR) Department of Chemistry, The University of Western Ontario, Chemistry Building, 1151 Richmond Street, London, Ontario N6A 5B7, Canada

∗ Corresponding author. Tel.: +1 519 661 2111x86161; fax: +1 519 661 3022; E-mail address: zfding@uwo.ca (Z. Ding); http://publish.uwo.ca/~zfding/

Abstract

With ongoing and expending global energy needs, nuclear power is likely to be a key energy source for many more generations. A key question is still the fate of spent nuclear fuel (SNF). SNF contains a great deal of valuable material. In order to improve safety and handling, herein is proposed relatively high melting point ionic liquid (IL) or organic ionic plastic crystals (OIPCs) for biphasic water|IL metal ion extraction. The proposed IL, tetraoctylphosphonium tetrakis(pentafluorophenyl)borate, $P_{8888}(C_6F_5)_4$, was discovered to have a melting point of ~55°C and a high degree of order by differential scanning calorimetry and X-ray diffraction, respectively. In this way, the IL/OIPC could be used in ligand assisted metal ion extraction from water solutions at elevated temperatures and then 'frozen' at ambient conditions for facile manipulation and transport of the SNF. To test the feasibility of this, electrochemistry such as cyclic voltammetry at a water|IL micro-interface (25 µm in diameter) was employed to assess the thermodynamics of K^+ ligand assisted transfer. It was revealed that the TRUEX (Transuranium Extraction) ligand octyl(phenyl)-N,N'-diisobutylcarbamoylphosphine oxide (CMPO) has a high to moderate coordination to K^+ at the w| $P_{8888}(C_6F_5)_4$, micro-interface. Two ligand to K^+ stoichiometries were determined to be 3:1 and 2:1, respectively.

1. Introduction

Ionic liquids (ILs) are salts, typically composed of large organic cations/anions, with melting points around ambient temperatures. They are favored over conventional solvents owing to their versatile and tunable properties – either through structural modification or by interchanging different cations and anions – such as large electrochemical stability, low vapor pressure, hydrophobicity, etc. [1-3]. ILs have been used in a wide variety of applications including battery electrolytes [4-6], solvent for nanoparticle synthesis [7], as antibacterial agents [8], etc. It has been shown that hydrophobic ILs are good candidates for metal ion extraction in biphasic, water|IL (w|IL) [9-12], systems. In metal ion extraction, a hydrophobic ligand is typically dissolved in the organic phase and coordinates with the metal ion either interfacially or in the bulk organic/aqeuous phase [13, 14]. Conventional means of separation have been through physical mixing of the two phases [9, 15]; however, as previously demonstrated [10-12, 16], this process can also be investigated electrochemically using liquid|liquid electrochemistry performed at a polarizable interface between two immiscible electrolytic solutions (ITIES) [13, 14, 17-21]. Furthermore, in order to reduce samples sizes and improve sensitivity, a micro-ITIES is often employed, such as at the tip of a pulled borosilicate glass capillary [11, 16, 22-24]. In this way, facilitated ion transfer (FIT) can be studied through the three generalized mechanisms, including transfer through interfacial complexation (TIC), aqueous complexation followed by transfer, and transfer followed by complexation (TOC), and aqueous complexation followed by transfer (ACT) [13, 14]. By studying these processes electrochemically, valuable thermodynamic parameters, such as the overall complexation constant, β, and metal ion:ligand stoichiometry (1:n) can be obtained [25]. These data are invaluable for the comparison of different ligand species and across varying biphasic systems, such as in the comparison of different w|IL combinations, but also in understanding the mechanisms of spent nuclear fuel (SNF) reprocessing [26].

After discharge from the reactor, nearly 95% of the fuel is usable uranium that is contaminated with various metals spanning the periodic table and poison the fission reaction; however, at present, only roughly half of all SNF is recycled [26]. It is beholden to find cheaper and more effective means for SNF recycling to make this process more attractive to reduce the amount of nuclear waste that is stored, either on the surface or in deep geological repositories.

An emerging class of compounds, often referred to as organic ionic plastic crystals (OIPCs), are similar to ILs in that they are large organic salts; however, the melting point of OIPCs is somewhat elevated relative to ILs and they typically have multiple solid-solid (*s-s*) phase transitions below the melt [27, 28]. While ILs have been shown to have better thermodynamics relative to traditional molecular solvents for metal extraction [9], these new materials could potentially offer similar chemical favorability while at the same time have the potential to 'freeze' SNF material after transfer, within the plastic phase, for safe handling and transport. Herein, we examine electrochemically, the facilitated IT of potassium with a traditional SNF ligand, octyl(phenyl)-N,N'-diisobutylcarbamoylphosphine oxide (CMPO), at w|IL interface. The IL, tetraoctylphosphonium tetrakis(pentafluorophenyl)borate ($P_{8888}B(C_6F_5)_4$) was prepared and its crystal structure was determined. $P_{8888}B(C_6F_5)_4$ was found to have a modest melting point of 55ºC by DSC analysis.

2. Experimental

2.1. Chemicals All purchased reagents were used as received, without purification and all aqueous solutions were made using MilliQ water ($\geq$18 MΩ cm). Potassium nitrate ($\geq$99.99%), trioctylphosphine (97%), 1-bromooctane (99%), dichloromethane ($\geq$99.5%) and tetramethylammonium sulfate ($\geq$99.0%) were obtained from Sigma-Aldrich (Mississauga, ON). Potassium tetrakis(pentafluorophenyl)borate (KB($C_6F_5)_4$, $\geq$99.9%) was sourced from

Boulder Scientific (Longmont, CO). Octyl(phenyl)-N,N'-diisobutylcarbamoylphosphine oxide (CMPO) was bought from Strem Chemicals Inc. (Newburyport, MA).

2.2. Ionic Liquid Preparation Tetraoctylphosphonium bromide ($P_{8888}Br$) ionic liquid was prepared through addition of trioctylphosphine and 1-bromooctane in a pressure tube (ACE glass, Vineland, NJ), with a stoichiometric excess of the bromoalkane and under an Ar atmosphere. A stir bar was added, the vessel closed and stirred for ~24 h. Afterwards, excess bromoalkane was removed under reduced atmosphere. Subsequently, the metathesis between $P_{8888}Br$ and $KB(C_6F_5)_4$ using stoichiometric equivalents was performed in DCM, in air, with stirring overnight to form the IL tetraoctylphosphonium tetrakis(pentafluorophenyl)borate ($P_{8888}(C_6F_5)_4$). $P_{8888}(C_6F_5)_4$ was recrystallized twice at –20°C in ethanol. After each step, the IL was structurally confirmed through ^{1}H-, ^{31}P-, and ^{19}F-NMR, as has been detailed elsewhere [3, 24, 29].

2.3. Electrochemistry All electrochemical experiments were conducted using a Modulab workstation (Ametek Advanced Measurement Technology, Farnborough, UK) and using a modified micropipette holder (HEKA Electronics, Mahone Bay, NS), 2.0 mm inner diameter, as has been described recently [10, 29]. Micropipettes, with a 25 µm diameter, 250-500 µm long, micro-channel situated at the tip, were fabricated as has been detailed previously [10, 29]. The micropipette as installed into the holder, which has an integrated silver wire connecting to the working electrode (WE) lead of the workstation, and then back filled with the aqueous solution using a syringe. The pipette was then immersed in the ionic liquid solution with the w|IL interfaced maintained at the tip with the aid of the syringe, which was carefully monitored using a CCD camera (Motic Inc., Richmond, BC) plus 12× zoom lens assembly (Navitar, Rochester, NY). Electrolytic cells shown in Scheme 2 were used.

$$\left| \text{Ag} \left| \text{AgNO}_3 \left| \begin{array}{c} 5 \text{ mM KNO}_3 \\ (aq) \end{array} \right\| \begin{array}{c} x \text{ mM CMPO} \\ (P_{8888}B(C_6F_5)_4) \end{array} \right| \text{Ag}(C_6F_5)_4 \left| \text{Ag} \right. \right. \qquad \text{Cell 1}$$

$$\left| \text{Ag} \left| \text{AgNO}_3 \right| \begin{array}{c} 0.5 \text{ mM (N(CH}_3)_4)_2\text{SO}_4 \\ 5 \text{ mM KNO}_3 \\ (aq) \end{array} \right\| P_{8888}B(C_6F_5)_4 \left| \text{Ag}(C_6F_5)_4 \right| \text{Ag} \qquad \text{Cell 2}$$
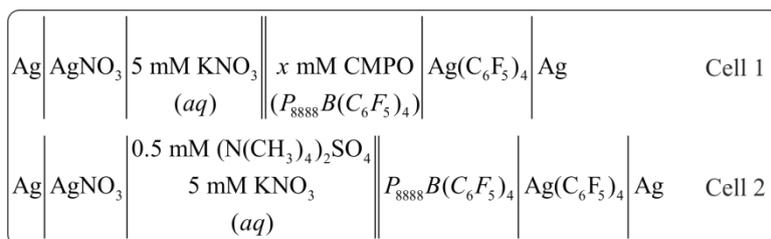
Scheme 2: Electrolytic cells employed, where CMPO is the ligand octyl(phenyl)-N,N'-diisobutylcarbamoylphosphine oxide, and $P_{8888}B(C_6F_5)_4$, is the ionic liquid tetraoctylphosphonium tetrakis(pentafluorophenyl)borate.

Unless otherwise stated, all electrochemical experiments were conducting using a heating mantle at 60 ℃.

2.4. X-ray Crystallography Samples were mounted on a Mitegen polyimide micromount with a small amount of Paratone N oil. The sample crystal was placed on the diffractometer at 273 K and cooled at a rate of 3 K min^{-1} until 150 K was reached. All X-ray measurements were made on a Nonius KappaCCD diffractometer at a temperature of 150 K. The unit cell dimensions were determined from a symmetry constrained fit of 9965 reflections with $5.64° < 2\theta < 49.64°$. The data collection strategy was a number of ω and φ scans which collected data up to 50.66° (2θ). The frame integration was performed using SAINT software [30]. The resulting raw data were scaled and absorption corrected using a multi-scan averaging of symmetry equivalent data using SADABS [31].

2.5. Differential Scanning Calorimetry (DSC) A DSC131evo (KEP Technologies group, Laxou, FR) was used for scanning calorimetric analysis, equipped with a cryothermostat cooling assembly with an operational range of –70 to 500 ℃. Scans in the range of –170 to 400 ℃ were generously performed by KEP Technologies using the same DSC instrument, with a liquid nitrogen cooled assembly installed. All samples were first heated to 150 ℃, then

cooled to the lower temperature threshold before heating, to ensure sample homogeneity. All samples were performed under a flow of inert N_2 gas.

3. Results and Discussion

3.1. Potential window at water|ionic liquid micro-interfaces

Figure 1A depicts the cyclic voltammograms obtained using Cell 1 without CMPO added at a scan rate (v) of 0.020 V s^{-1}. For this blank case, the sharp increase (at positive potentials) or decrease (at negative potentials) marks the edge of the polarizable potential window (PPW), which is limited by the transfer of the supporting electrolyte/analyte from the aqueous phase, or the anionic/cationic component of the IL phase. For example, at the positive end this is either K^+ transfer for aqueous to IL (w to IL) or the anionic component of the IL, $B(C_6F_5)_4^-$, from IL to w; while at the negative end, this is either NO_3^- from w to IL or P_{8888}^+ from IL to w. Owing to the extreme hydrophobicity of the IL components [3, 32], it is likely that change in current is due to K^+ and NO_3^- transfer.
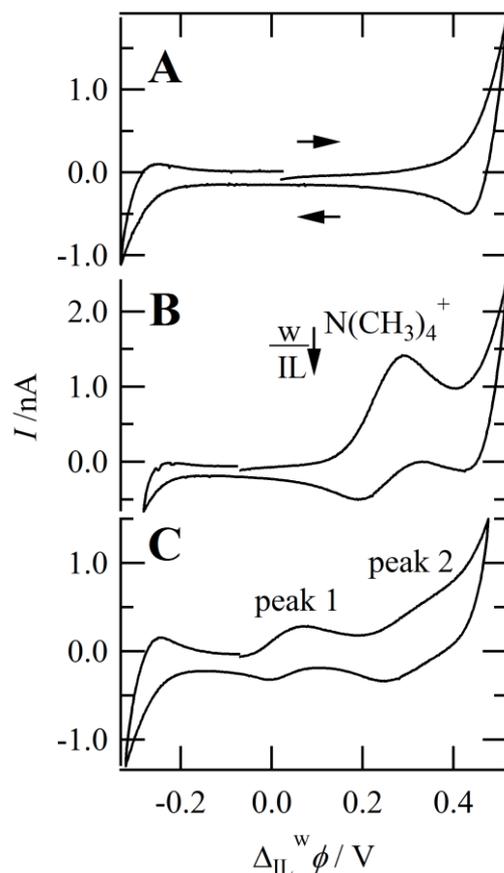
Figure 1: Cyclic voltammograms obtained at a w|P$_{8888}$B(C$_6$F$_5$)$_4$, 25 μm diameter, micro-interface housed at the tip of a pulled capillary using (**A**) Cell 1, without CMPO added, (**B**) Cell 2, and (**C**) Cell 1 with $y = 60$ mM of CMPO added to the IL phase. All traces were obtained at a scan rate of 0.020 V s^{-1} and with a heating mantle at 60 °C.

In Figure 1B, using Cell 2, when the potential was swept from negative to positive potentials, a peak-shaped wave indicative of N(CH$_3$)$_4^+$ transfer from w to IL was observed at a peak potential of 0.298 V. Upon reversal of the scan direction, a second peak-shaped wave can be seen at 0.170 V and is the result of N(CH$_3$)$_4^+$ transfer back from IL to w. These peak-shaped ion transfer (IT) waves are owing to two factors: (1) the geometric confinement of the aqueous phase within the micro-channel of the pulled pipette for the w to IL transfer wave; (2) the high viscosity, i.e. low diffusion coefficient, in the IL phase for the IL to w transfer wave. For the former, the small volume of solution – relative to the interfacial size – means

that $N(CH_3)_4^+$ ions in the vicinity of the interface are consumed faster than they can diffuse from higher up in the micro-channel; this is also called 'linear diffusion', and gives rise to a peak-shaped signal rather than a steady-state voltammogram typical of solid microelectrodes [29, 33]. The low diffusion coefficient generates a similar linear diffusion-based response in the IL to w transfer. This is in good agreement with previous reports in the literature [10, 12-14, 29, 32].

All IT potentials were referenced relative to $N(CH_3)_4^+$ transfer using a formal IT potential, $\Delta_{IL}^{w}\phi^{o'}$, of 0.270 V [29]. In turn, half-wave potentials, $\Delta_{IL}^{w}\phi_{1/2}$, were calculated using the peak potential $\Delta_{IL}^{w}\phi_p$, from the w to IL transfer wave and the following:

$$\Delta_{IL}^{w}\phi_{1/2} = \Delta_{IL}^{w}\phi_p + 0.028 \text{ V}/z \text{ [34]}.$$
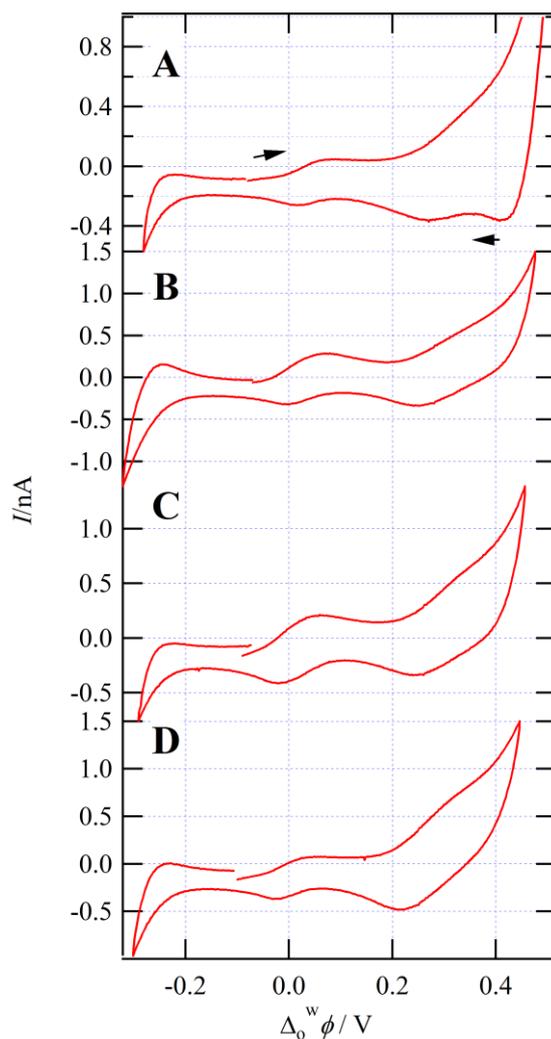
Figure 2: Cyclic voltammograms recorded using Cell 1 with the concentration of CMPO (*y*) varied in the IL phase from 30 to 85 mM from A to D. All other instrument parameters were the same as detailed in Figure 1.

3.2. Facilitated ion transfer of K^+ with CMPO at w/IL micro-interface

Moving forward, with the addition of the ligand octyl(phenyl)-N,N'-diisobutylcarbamoylphosphine oxide (CMPO) to Cell 1, two new transfer waves developed with $\Delta_{IL}^{w}\phi_{1/2}$ equal to 0.043 and 0.333 V for peak 1 and 2, as noted in Figure 1C, respectively. Since CMPO is quite hydrophobic and neutral, it can be concluded that these peaks are the facilitated ion transfer waves for the coordination of CMPO to K^+. With this in mind, the

thermodynamics of K-CMPO$_n^{z+}$ facilitated ion transfer, where n is the ligand stoichiometry, was investigated by changing the concentration of CMPO in the IL phase from 20 to 90 mM; CVs were recorded for each iteration, see Figure 2. $\Delta_{IL}^{w}\phi_{1/2}$ for the two transfer waves were seen to shift from 0.156 to 0.027 V for peak 1, and from 0.361 to 0.313 V for peak 2. These results agree well with the analytical treatment of facilitated ion transfer [25], as recently demonstrated [10, 12, 24] and reviewed [13, 14]. Using the analytical treatment for facilitated ion transfer, $\Delta_{IL}^{w}\phi_{1/2}$ versus concentration profiles [25], as shown in equation 2, two valuable thermodynamic constants for this reaction can be obtained, including n, and the overall complexation constant β.

$$-z\mathrm{F}/(\mathrm{RT})\left(\Delta_{IL}^{w}\phi_{1/2} - \Delta_{IL}^{w}\phi_{\mathrm{K}^+}^{o'}\right) = n\ln(c_{\mathrm{CMPO}}^{*}) + \ln(\beta) + \ln(\xi) \tag{2}$$

here, z, F, R, and T have their usual significance, while $\Delta_{IL}^{w}\phi_{\mathrm{K}^+}^{o'}$ is the formal IT potential of K$^+$ at the w|P$_{8888}$B(C$_6$F$_5$)$_4$ interface; this was estimated to be ~0.600 V based on that determined for K$^+$ at the w|P$_{66614}$B(C$_6$F$_5$)$_4$ interface [35]. P$_{66614}$B(C$_6$F$_5$)$_4$ is the IL trihexyltetradecylphosphonium tetrakis(pentafluorophenyl)borate, which is a structural isomer of the IL used here. c_{CMPO}^{*} is the initial CMPO concentration and $\xi = \sqrt{D_{i,IL}/D_{i,w}}$. ξ was estimated by using the diffusion coefficient of decamethylferrocene in P$_{8888}$B(C$_6$F$_5$)$_4$, 3×10^{-8} cm^2 s^{-1} [29], and a value of 1×10^{-5} cm^2 s^{-1} in the aqueous phase. In this way, n can be obtained from the slope of a linear fitting, and β from the y-intercept.

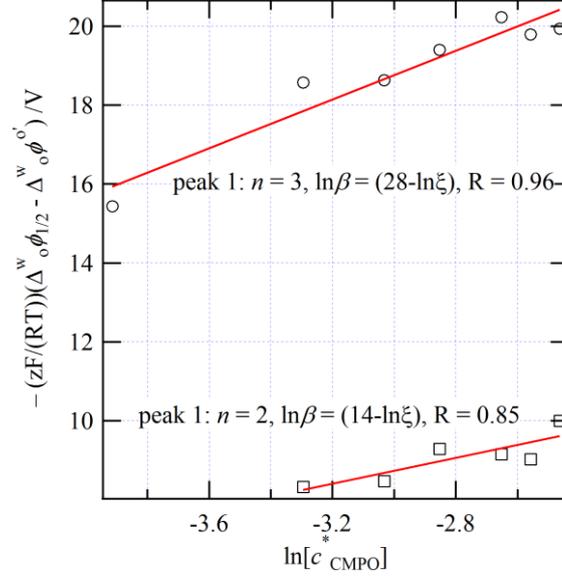**Figure 3:** Trend of $-z\mathrm{F}/(\mathrm{RT})(\Delta_{IL}^{w}\phi_{\mathrm{ML}_n^z,1/2} - \Delta_{IL}^{w}\phi^{o'})$ versus ln[c$_{CMPO}$] obtained from the shift in $\Delta_{IL}^{w}\phi_{\mathrm{ML}_n^z,1/2}$ (see Figure 2). Red traces indicate the linear curve fitting applied to the data with metal:ligand (1:n) stoichiometry, overall complexation constant β ($\xi = \sqrt{D_{IL}/D_w}$), and Pearson's R values indicated.

The linear trend of $-z\mathrm{F}/(\mathrm{RT})\left(\Delta_{IL}^{w}\phi_{1/2} - \Delta_{IL}^{w}\phi_{\mathrm{K}^+}^{o'}\right)$ versus $\ln(c_{CMPO}^*)$ has been plotted in Figure 3 for the two facilitated IT waves observed in Figure 2 with a linear regression analysis applied to each – red traces. This analysis revealed an n of 3 and 2 with a lnβ of 30 and 16, for peaks 1 and 2, respectively. Owing to the estimation of $\Delta_{IL}^{w}\phi_{\mathrm{K}^+}^{o'}$ and ξ, these values should be taken as estimates; however, this provides a qualitative indicator of the ligand strength in a w|IL biphasic system for K$^+$ extraction with CMPO. These results are in good agreement with recent reports by our group [11, 32] and others [12]. The overall β for K-CMPO$_3^+$ facilitated IT shown here, is several orders of magnitude less than that for Sr-CMPO$_3^{2+}$. However, K-CMPO$_3^+$ is in the same potential region as that shown by Nishi *et al*. [12] for K$^+$ transfer facilitated by dibenzo-18-crown-6 ether (DB18c6), using a water| *N*-octadecylisoquinolinium tetrakis(3,5-bis(trifluoromethyl)phenyl)borate IL interface, providing a 1:1, K$^+$:DB18c6 ratio.

This would indicate that, since 3 CMPOs are required versus 1 DB18c6 for roughly the same order of magnitude for β, CMPO has less of an affinity for K^+.

Nevertheless, these results indicate that potassium extraction into an IL phase using traditional SNF ligands is feasible. Indeed, according to our recent studies of CMPO coordination to Cs^+ [10], Rb^+ [36], and Sr^{2+} [11] – all of which are major components of SNF [26] – at the $w|P_{66614}B(C_6F_5)_4$ interface, indicates a strong affinity for this ligand to the selected ions. If the $w|P_{66614}B(C_6F_5)_4$ interface is considered roughly equivalent to the $w|P_{8888}B(C_6F_5)_4$ one, then a qualitative trend can be established for CMPO-M^{z+} complexation of increasing strength as: $Rb^+>K^+\approx Cs^+>Sr^{2+}$.

3.3. Differential scanning calorimetry

Figure 4 illustrates the differential scanning calorimetric (DSC) traces obtained for tetraoctylphsophonium bromide ($P_{8888}Br$) and tetraoctylphosphonium tetrtakis(pentafluorophenyl)borate ($P_{8888}B(C_6F_5)_4$) ILs. The green and blue curves show the heat flow profiles with sample temperature for $P_{8888}Br$ at temperature ramps of 10 and 2 ℃ min^{-1}, respectively. For the former, 2 solid-solid (*s-s*) phase transitions can be resolved at 12 and 16 ℃, along with a temperature of melting at 38 ℃. Reducing the temperature ramp improves the resolution of these peaks [37], as can be observed in the blue trace in Figure 4 [37]. Here, a glass transition, T_g, along with the *s-s* transitions were recorded at –7, 9, and 22 ℃, with a temperature of fusion at 42 ℃. In this sense, $P_{8888}Br$ could behave as an excellent material for biphasic metal extraction; whereby, ions could be transferred through biphasic, w|IL, mixing at an elevated temperature, and after separation, the IL phase could be 'frozen' at room temperature for easy storage and handling.

Owing to the hydrophilic nature of Br^-, it is likely to leach into the aqueous phase as was shown recently [38]; however, this may be advantageous if Br^- was used as a sacrificial

anion and replaced by the in-coming metal anion, such as pertechnetate, TcO_4^- [39]. This being said, the strategy presented here was to preserve the IL intact and for this to be possible, the w|IL interface must be polarizable; hence, Br^- was exchanged for $B(C_6F_5)_4^-$, which has been shown to be hydrophobic [32] as well as electrochemically stable [40].

After replacing Br^- with $B(C_6F_5)_4^-$, through a metathesis reaction with $KB(C_6F_5)_4$, the resultant IL becomes more crystalline, as can be seen in the black trace in Figure 4. The $P_{8888}B(C_6F_5)_4$ thermogram at a $10ºC\,min^{-1}$ ramp, shows one phase transition at 55ºC corresponding to the temperature of melting; this result indicates that $P_{8888}B(C_6F_5)_4$ has a higher order of crystallinity than the $P_{8888}Br$ precursor IL. This is likely owing to the highly symmetrical nature of both cation and anion.
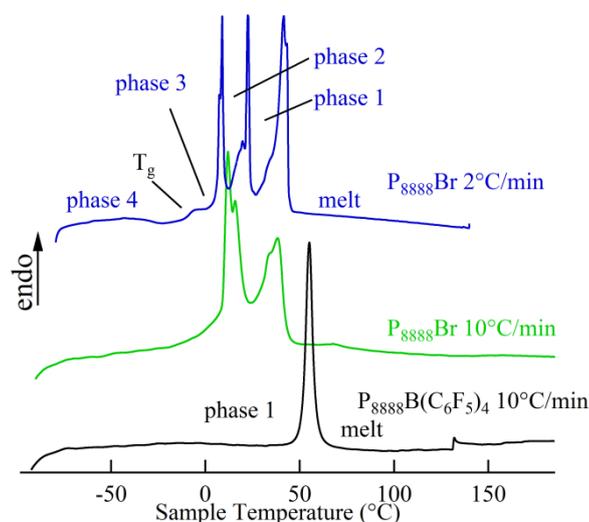

Figure 4: Differential Scanning Calorimetric traces for the ILs $P_{8888}Br$ and $P_{8888}B(C_6F_5)_4$ scanned from negative to positive temperatures at a temperature ramp as indicated.

3.4. Crystal structure of $P_{8888}B(C_6F_5)_4$

The molecular structure of $P_{888}B(C_6F_5)_4$ was determined by single crystal X-ray crystallography. The cation and anion are depicted in Figure 5A and B respectively (see SI for details). Suitable crystals were obtained through recrystallization from hexane and were found

to crystallize in the triclinic space group P -1. The phosphorous atom shows pronounced anisotropic displacements which propagate through two of the n-octyl chains. Two atoms in each of these two chains were distributed over 2 sites. In these cases, the secondary site name was designated with a prime (') character. The atoms with distinct secondary sites were C31', C33', C42', and C43'. The normalized occupancies for the secondary sites refined to the following values: 0.318(7) for C31' and C33' and 0.509(14) for C42' and C43'. The P-C bond lengths ranged from 1.67 to 1.99 Å which agree well with previous tetraalkylphosphonium salts [41]. For additional information see the Supplementary Data, Tables S1-S6.
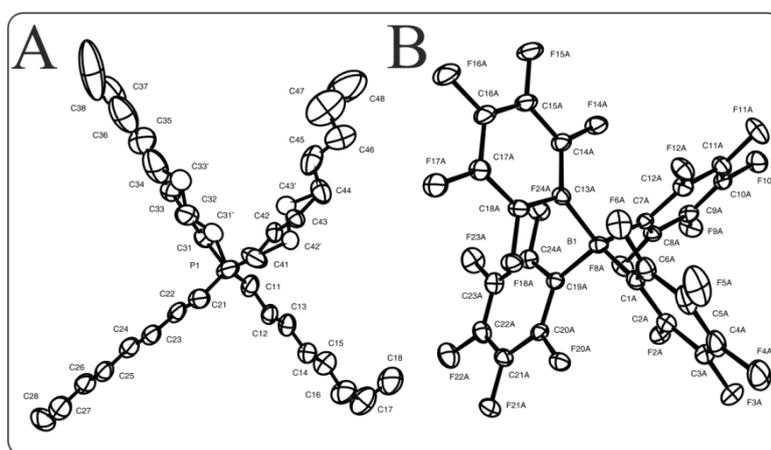

Figure 5: Structure of $P_{8888}B(C_6F_5)_4$ ($C_{56}H_{68}BF_{20}P$) as determined by X-ray diffraction. (**A**) Oak Ridge Thermal Ellipsoid Plot (ORTEP) of P_{8888}^+ showing naming and numbering scheme. Ellipsoids are at the 50% probability level and hydrogen atoms were omitted for clarity. The disordered portion of the cation is depicted as "open" ellipsoids and bonds. (**B**) ORTEP of $B(C_6F_5)_4^-$ showing naming and numbering scheme. Ellipsoids are at the 25% probability level for clarity.

Since it is difficult to truly 'freeze' OIPCs in order to obtain a clear X-ray diffraction pattern [42], it is unlikely that $P_{8888}B(C_6F_5)_4$ is one; rather, it is simply a relatively high melting point IL with a high level of order below 55 ℃. This does not, however, preclude its use in trapping metal ions by freezing them within its crystal lattice or below its T_g. This

would necessarily introduce defects into the final ionic lattice, lowering the overall melting point, and is something we are currently investigating; however, this is beyond the scope of the present report.

4. Conclusions

Herein, the metal ion extraction of K^+ has been proposed using a traditional SNF ligand, CMPO, at a w|IL interface. The IL, $P_{8888}B(C_6F_5)_4$, whose crystal structure was identified as triclinic, P –1, has been used at elevated temperatures, 60 ℃, to study the ligand-assisted transfer electrochemically at a w|$P_{8888}B(C_6F_5)_4$ micro-interface. This analysis showed two FIT waves, observed using cyclic voltammetry. After a facile concentration study and comparison to known analytical treatments [25], the two waves were evidenced to have K^+:CMPO stoichiometries of 1:3 and 1:2 and overall complexation constants of 1×10^{13} and 8.9×10^6 L mol^{-1}, respectively. This is comparable to other metal ion-ligand coordination strengths and provides a vital route to compare different metal-ligand or biphasic systems.

The DSC and X-ray diffraction results for $P_{8888}B(C_6F_5)_4$ show a highly ordered system with a relatively high melting point of 55 ℃. Such a system would be an interesting substitute for current SNF storage materials. A biphasic extraction could be conducted a reasonably elevated temperatures, then cooled for easy storage and handling. This would be even more interesting if captured metals could be retained in the IL glass phase, where they could be later retrieved by gentle heating and reverse biphasic extraction. It is recognized that any metal ions would introduce defects into the crystal lattice or the IL glass phase, altering the thermal profile of the IL; nevertheless, this is an interesting route to SNF short term storage. While beyond the scope of the present article, work is ongoing towards this aspect.

References

[1] Y.-H. Tian, G.S. Goff, W.H. Runde, E.R. Batista, Exploring Electrochemical Windows of Room-Temperature Ionic Liquids: A Computational Study, J. Phys. Chem. B, 116 (2012) 11943-11952.

[2] D.R. MacFarlane, N. Tachikawa, M. Forsyth, J.M. Pringle, P.C. Howlett, G.D. Elliott, J.H. Davis, M. Watanabe, P. Simon, C.A. Angell, Energy applications of ionic liquids, Energy Environ. Sci., 7 (2014) 232-250.

[3] T.J. Stockmann, R. Guterman, P.J. Ragogna, Z. Ding, Trends in Hydrophilicity/Lipophilicity of Phosphonium Ionic Liquids as Determined by Ion-Transfer Electrochemistry, Langmuir, 32 (2016) 12966–12974.

[4] T.J. Simons, M. Salsamendi, P.C. Howlett, M. Forsyth, D.R. MacFarlane, C. Pozo-Gonzalo, Rechargeable Zn/PEDOT Battery with an Imidazolium-Based Ionic Liquid as the Electrolyte, ChemElectroChem, 2 (2015) 2071-2078.

[5] C. Pozo-Gonzalo, C. Virgilio, Y. Yan, P.C. Howlett, N. Byrne, D.R. MacFarlane, M. Forsyth, Enhanced performance of phosphonium based ionic liquids towards 4 electrons oxygen reduction reaction upon addition of a weak proton source, Electrochem. Commun., 38 (2014) 24-27.

[6] S. Higashi, Y. Kato, K. Takechi, H. Nakamoto, F. Mizuno, H. Nishikoori, H. Iba, T. Asaoka, Evaluation and analysis of Li-air battery using ether-functionalized ionic liquid, J. Power Sources, 240 (2013) 14-17.

[7] J. Gao, R.S. Ndong, M.B. Shiflett, N.J. Wagner, Creating Nanoparticle Stability in Ionic Liquid [C4mim][BF4] by Inducing Solvation Layering, ACS Nano, 9 (2015) 3243-3253.

[8] M. Zakrewsky, K.S. Lovejoy, T.L. Kern, T.E. Miller, V. Le, A. Nagy, A.M. Goumas, R.S. Iyer, R.E. Del Sesto, A.T. Koppisch, D.T. Fox, S. Mitragotri, Ionic liquids as a class of materials for transdermal delivery and pathogen neutralization, Proc. Natl. Acad. Sci, 111 (2014) 13313-13318.

[9] S. Dai, Y.H. Ju, C.E. Barnes, Solvent extraction of strontium nitrate by a crown ether using room-temperature ionic liquids, J. Chem. Soc., Dalton Trans., (1999) 1201-1202.

[10] T.J. Stockmann, J. Zhang, A.-M. Montgomery, Z. Ding, Electrochemical assessment of water|ionic liquid biphasic systems towards cesium extraction from nuclear waste, Anal. Chim. Acta, 821 (2014) 41-47.

[11] T.J. Stockmann, Y. Lu, J. Zhang, H.H. Girault, Z. Ding, Interfacial Complexation Reactions of Sr2+ with Octyl(phenyl)-N,N-diisobutylcarbamoylmethylphosphine Oxide for Understanding Its Extraction in Reprocessing Spent Nuclear Fuels, Chem. Eur. J., 17 (2011) 13206-13216.

[12] N. Nishi, H. Murakami, S. Imakura, T. Kakiuchi, Facilitated transfer of alkali-metal cations by dibenzo-18-crown-6 across the electrochemically polarized interface between an aqueous solution and a hydrophobic room-temperature ionic liquid, Anal. Chem., 78 (2006) 5805-5812.

[13] Z. Samec, J. Langmaier, T. Kakiuchi, Charge-transfer processes at the interface between hydrophobic ionic liquid and water, Pure Appl. Chem., 81 (2009) 1473-1488.

[14] P. Peljo, H.H. Girault, Electrochemistry at Liquid/Liquid Interfaces, Encyclopedia of Analytical Chemistry, John Wiley & Sons, Ltd2012.

[15] X. Sun, H. Luo, S. Dai, Ionic Liquids-Based Extraction: A Promising Strategy for the Advanced Nuclear Fuel Cycle, Chem. Rev., 112 (2011) 2100-2128.

[16] U. Nestor, H. Wen, G. Girma, Z. Mei, W. Fei, Y. Yang, C. Zhang, D. Zhan, Facilitated Li+ ion transfer across the water/1,2-dichloroethane interface by the solvation effect, Chem. Commun., 50 (2014) 1015-1017.

[17] M.M. Hossain, C.S. Kim, H.J. Cha, H.J. Lee, Amperometric Detection of Parathion and Methyl Parathion with a Microhole-ITIES, Electroanalysis, 23 (2011) 2049-2056.

[18] M.A. Deryabina, S.H. Hansen, H. Jensen, Versatile Flow-Injection Amperometric Ion Detector Based on an Interface between Two Immiscible Electrolyte Solutions: Numerical and Experimental Characterization, Anal. Chem., 83 (2011) 7388-7393.

[19] Y.F. Zhao, Y.Q. Gao, D.P. Zhan, H. Liu, Q. Zhao, Y. Kou, Y.H. Shao, M.X. Li, Q.K. Zhuang, Z.W. Zhu, Selective detection of dopamine in the presence of ascorbic acid and uric acid by a carbon nanotubes-ionic liquid gel modified electrode, Talanta, 66 (2005) 51-57.

[20] H. Nagatani, H. Sakae, T. Torikai, T. Sagara, H. Imura, Photoinduced Electron Transfer of PAMAM Dendrimer–Zinc(II) Porphyrin Associates at Polarized Liquid|Liquid Interfaces, Langmuir, 31 (2015) 6237-6244.

[21] Q. Duong, Y. Tan, J. Corey, S. Anz, P. Sun, Mechanism of the Transfer of AuCl4– and TOA+ Ions Across the Liquid/Liquid Interface, J. Phys. Chem. C, 119 (2015) 10365-10369.

[22] Y. Qiao, B. Zhang, X. Zhu, T. Ji, B. Li, Q. Li, E. Chen, Y. Shao, Facilitated Ion Transfers at the Micro-Water/1,2-Dichloroethane Interface by Crown Ether Derivatives, Electroanalysis, 24 (2013) 1080-1084.

[23] S. Liu, Q. Li, Y. Shao, Electrochemistry at micro- and nanoscopic liquid/liquid interfaces, Chem. Soc. Rev., 40 (2011) 2236-2253.

[24] T.J. Stockmann, J.-M. Noel, A. Abou-Hassan, C. Combellas, F. Kanoufi, Facilitated Lewis Acid Transfer by Phospholipids at a (water|CHCl3) Liquid|liquid Interface Towards Biomimetic and Energy Applications, J. Phys. Chem. C, 120 (2016) 11977–11983.

[25] F. Reymond, G. Lagger, P.-A. Carrupt, H.H. Girault, Facilitated ion transfer reactions across oil|water interfaces. Part II. Use of the convoluted current for the calculation of the

association constants and for an amperometric determination of the stoichiometry of MLjz+ complexes, J. Electroanal. Chem., 451 (1998) 59-76.

[26] J. Bruno, R.C. Ewing, Spent nuclear fuel, Elements, 2 (2006) 343-349.

[27] L. Jin, P.C. Howlett, J.M. Pringle, J. Janikowski, M. Armand, D.R. MacFarlane, M. Forsyth, An organic ionic plastic crystal electrolyte for rate capability and stability of ambient temperature lithium batteries, Energy Environ. Sci., 7 (2014) 3352-3361.

[28] U.A. Rana, R. Vijayaraghavan, D.R. MacFarlane, M. Forsyth, Plastic crystal phases with high proton conductivity, J. Mater. Chem., 22 (2012) 2965-2974.

[29] T.J. Stockmann, Z. Ding, Tetraoctylphosphonium Tetrakis(pentafluorophenyl)borate Room Temperature Ionic Liquid toward Enhanced Physicochemical Properties for Electrochemistry, J. Phys. Chem. B, 116 (2012) 12826-12834.

[30] Bruker-Nonius, SAINT version 2012.12, Bruker-Nonius, Madison, WI 53711, USA, 2012.

[31] Bruker-Nonius, SADABS version 2012.1, Bruker-Nonius, Madison, WI 53711, USA, 2012.

[32] T.J. Stockmann, A.-M. Montgomery, Z. Ding, Determination of alkali metal ion transfers at liquid|liquid interfaces stabilized by a micropipette, J. Electroanal. Chem., 684 (2012) 6-12.

[33] R.M. Wightman, Microvoltammetric electrodes, Anal. Chem., 53 (1981) 1125A-1126, 1128A, 1130A, 1132A, 1134A.

[34] A.J. Bard, L.R. Faulkner, Electrochemical Methods: Fundamentals and Applications, 2nd ed., John Wiley, New York, 2001.

[35] T.J. Stockmann, Z. Ding, Facile determination of formal transfer potentials for hydrophilic alkali metal ions at water|ionic liquid microinterfaces, Phys. Chem. Chem. Phys., 14 (2012) 13949-13954.

[36] T.J. Stockmann, A.-M. Montgomery, Z. Ding, Correlation of Stoichiometries for Rb+ Extraction Determined by Mass Spectrometry and Electrochemistry at Liquid|Liquid Interfaces, Anal. Chem., 84 (2012) 6143-6149.

[37] M. Forsyth, J.M. Pringle, D.R. MacFarlane, Ion Conduction in Organic Ionic Plastic Crystals, Electrochemical Aspects of Ionic Liquids, John Wiley & Sons, Inc.2011, pp. 347-373.

[38] M.L. Dietz, D.C. Stepinski, Anion concentration-dependent partitioning mechanism in the extraction of uranium into room-temperature ionic liquids, Talanta, 75 (2008) 598-603.

[39] I.A. Shkrob, T.W. Marin, D.C. Stepinski, G.F. Vandegrift, III, J.V. Muntean, M.L. Dietz, Extraction and Reductive Stripping of Pertechnetate from Spent Nuclear Fuel Waste Streams, Sep. Sci. Technol., 46 (2011) 357-368.

[40] W.E. Geiger, F. Barrière, Organometallic Electrochemistry Based on Electrolytes Containing Weakly-Coordinating Fluoroarylborate Anions, Acc. Chem. Res., 43 (2010) 1030-1039.

[41] G. Adamova, R.L. Gardas, M. Nieuwenhuyzen, A.V. Puga, L.P.N. Rebelo, A.J. Robertson, K.R. Seddon, Alkyltributylphosphonium chloride ionic liquids: synthesis, physicochemical properties and crystal structure, Dalton Trans., 41 (2012) 8316-8332.

[42] L. Jin, K.M. Nairn, C.M. Forsyth, A.J. Seeber, D.R. MacFarlane, P.C. Howlett, M. Forsyth, J.M. Pringle, Structure and Transport Properties of a Plastic Crystal Ion Conductor: Diethyl(methyl)(isobutyl)phosphonium Hexafluorophosphate, J. Am. Chem. Soc., 134 (2012) 9688-9697.